AIMS Mathematics, 5(3): 2009–2026.
DOI: 10.3934/math.2020133
Received: 28 September 2019
Accepted: 09 February 2020
Published: 21 February 2020

http://www.aimspress.com/journal/Math

Research article

Entropy Analysis for boundary layer Micropolar fluid flow

Paresh Vyas, Rajesh Kumar Kasana and Sahanawaz Khan*

Department of Mathematics, University of Rajasthan, Jaipur-302004, India

* **Correspondence:** Email: rkasanamaths@gmail.com; Tel: +01412708392.

Abstract: This paper reports entropy generation analysis of radiative micropolar fluid flow in porous medium. The mathematical model depicting convective boundary layer flow due to a vertically moving infinite plate bounding the porous medium on one side is solved numerically. An implicit finite difference method together with Gauss elimination method is used. The numerically computed velocity and temperature fields are employed to analyze entropy. The plots for entropy generation number for various sets of parameters are drawn. It is found that entropy generation number Ns decreases with increasing values of heat sink parameter Q and radiation parameter N whereas it increases with increasing values of Grashoff number Gr, Brinkman number Br. The Bejan number shows pronounced variations for the parameters entering into the problem.

Keywords: micropolar fluid; porous medium; entropy
Mathematics Subject Classification: 74A15, 76D10, 76S05

Nomenclature: Be: Bejan number; Br: Brinkman number; c_p: specific heat at constant pressure; Ec: Eckert number; g: acceleration due to gravity; Gr: Grashoff number; J: microinertia density; k: thermal conductivity; K: permeability of the porous medium; n: parameter related to microgyration vector and shear stress; N: radiation parameter; Ns: entropy generation number; Pr: Prandtl number; q: heat flux; q_r: radiation heat flux; Q: suction/injection parameter; S_G: local volumetric rate of entropy; S_{G_0}: characteristic entropy generation rate; T: temperature; u^*, v^*: components of velocities along and perpendicular to the plate, respectively; U_0: scale of free stream velocity; V_0: uniform normal velocity; x^*, y^*: distances along and perpendicular to the plate, respectively; **Greek symbols:** β: coefficient of volumetric thermal expansion of the fluid; γ: spin-gradient viscosity; δ: mean absorption constant; θ: dimensionless temperature; μ: fluid dynamics viscosity; μ_r: coefficient of vortex (microrotation) viscosity; σ: Stephan-Boltzman constant; ρ: fluid density; ϑ: fluid kinematic viscosity; ϑ_r: fluid kinematic rotational viscosity; w: angular velocity vector; Ω: dimensionless

temperature difference; **Subscripts:** ∞: free stream condition; **Superscripts:** $*$: dimensional properties; $(\,)'$: differentiation with respect to η

1. Introduction

The realm of micropolar fluid theory developed by Eringen [1] is important as it deals with the fluids with microstructures. The Navier–Stokes equations address fluid flow by treating fluid, a continuum. However, when the flow system is treated on micro scale, then the classical Navier–Stokes equations may fail to fully account for fluid transport, simply because in the Navier–Stokes equations, molecular spin is not accounted for. In fact, when the flow scale is of the same order as of the molecular size, the molecules spinning alter the flow field qualitatively and quantitatively. In that case, one needs to consider microcontinuum flow. In fact, Eringen's microcontinuum theory is a breakthrough for providing a mathematical basis to modify Navier–Stokes equations for microfluidics. In micropolar fluid theory, a micropolar fluid is considered as a continuous collection of finite-size particles, and there is an additional equation that accounts for the rotation of the microstructure. In fact, micropolar fluids are subclass of polar fluids (fluids with non-symmetric stress tensor) where the deformation of fluid elements is not taken into account. The micropolar fluid theory finds significance when the flow domain is of micro scale or nano scale. For example in channel flows, hydrodynamic quantities derived from Navier–Stokes equations do not match with experimental results, and the deviation mounts in cases of flow through narrow channels. Owing to real world applications, the microfluidics has emerged as a vibrant research domain. This includes modeling of the system as a design tool, and devising tool for solution strategies in case of mathematical models. Numerous studies have been reported on transport phenomenon of micropolar fluid in variety of configurations having technological applications. The theory of micropolar fluid and its extension to thermomicropolar fluids [2] may form suitable Non-Newtonian fluid models which can be used to analyze the behavior of exotic lubricants [3,4], shear flow [5], liquid crystals [6,7]. Kolpashchikov et al. [8] had derived a method to measure micropolar parameters experimentally. Ariman et al. [9,10] have presented a detailed review on micropolarfluid mechanics and applications. There have been some pertinent studies in different geometries pertaining to micropolar fluid [11–21].

Thermofluidics due to moving surface is important in understanding many natural phenomenon, and has many industrial applications. To be specific, processes such as fiber drawing, hot rolling, hot extrusion etc., involve heat transfer between moving surface and the surrounding fluid.

Given the wide array of applications, the problem of fluid flow due to a moving surface has been studied for variety of fluids. These theoretical studies cited in the ensuing text and the references contained therein offered a theoretical understanding of the phenomenon involved. This led to a want for solution strategies to handle the relevant mathematical models also.

Cess [22] examined thermal radiation with free convection. Hayday et al. [23] discussed free convection from a vertical plate with step discontinuities in surface temperature. Kao [24] examined heat transfer along a vertical plate with step jump. Cheng and Minkowycz [25] investigated heat transfer due to a vertical plate embedded in a porous medium. Raptis and Kafousias [26] reported the effect of magnetic field on heat transfer in porous medium fluid flow system bounded by an infinite vertical plate. Bianchi and Viskanta [27] investigated heat transfer on a continuous flat surface in a counter flow. Takhar et al. [28] investigated radiative MHD free convection of a gas past a

semi-infinite vertical plate. Chamkha [29] discussed unsteady MHD convective heat and mass transfer due to a moving plate with heat absorption. Abdelkhalek [30] employed perturbation method to derive heat and mass transfer in convective flow due to a moving vertical surface. Makinde [31] offered similarity solution for convective flow due to a moving surface with internal heat generation and convective boundary condition. Srinivasacharya and Surender [32] derived non-similar solution for a convective nanofluid flow past a vertical plate in a doubly stratified porous medium. Khalid et al. [33] examined heat transfer in ferrofluid with cylindrical shape nanoparticles past a vertical plate subjected to ramped wall temperature embedded in a porous medium. Mishra et al. [34] examined free convective micropolar fluid flow and heat transfer over a shrinking sheet with heat source. Chen and Liu [35] employed the least square spectral collocation method for nonlinear radiative heat transfer in moving porous plate. These studies were primarily focused on first law of thermodynamics, and did not looked into second law of thermodynamics.

We know that the second law of thermodynamics offers a window to gauge inherent thermodynamic irreversibility which is related to thermodynamic efficiency. Thermodynamic efficiency is a challenging aspect for designing pertinent equipment where efficient energy usage is a primary concern. The endeavors of entropy management have gained currency in thermofluidics after the path breaking work of Bejan [36,37]. He had shown that thermofluidic systems could be treated for entropy aspects, and given a formulation for computing local volumetric rate of entropy generation. Taking a clue, theoretical entropy analysis of fluid systems has emerged as a vibrant field of research. Many relevant studies have been reported in the literature. These include various types of configurations e.g., theoretical and experimental, varied geometries for variety of fluids, different end conditions and assumptions.

Srinivasacharya and Hima Bindu [42] studied entropy generation of micropolar fluid flow through concentric cylinder annulus with slip and convective boundary conditions. In another paper, Srinivasacharya and Hima Bindu [43] reported a theoretical study on entropy generation of micropolar fluid flow in an inclined porous pipe with convective boundary conditions. Asha and Deepa [44] investigated entropy generation for peristaltic blood flow of magneto-micropolar fluid with thermal radiation with tapered asymmetric channel. Sahin [45] investigated entropy generation for a viscous fluid flow in a duct subjected to constant surface temperature. Murthy and Srinivas [46] examined entropy generation analysis for micropolar fluid between two horizontal parallel plates of a channel with constant temperature. The effect of thermal radiation on entropy generation due to micropolar fluid flow along a wavy surface was investigated by Chen et al. [47]. Many other authors [48–57] and references contained therein have reported relevant studies.

The study undertaken here may find applications in chemical, automobile and other industries where varied polymeric suspensions, lubricants, paints, colloids etc. can be viewed as micropolar fluid. In this backdrop, the study presented here is pertinent to offer an elegant solution strategy for entropy generation analysis for boundary layer flow of a micropolar fluid in porous medium.

2. Mathematical model

Let us take a steady, laminar, incompressible 2-D radiative boundary layer flow of a micropolar fluid past a flat infinite plate moving vertically upwards embedded in a fluid saturated porous medium. The plate is perfectly attached with the porous medium bounding it on one side. The fluid is absorbing and emitting non-scattering radiation without phase change. The plate is subjected to a

uniform heat flux and a uniform suction. We choose a Cartesian coordinate system to schemate the problem where x*, y*-axes are chosen along the plate and normal to it respectively.

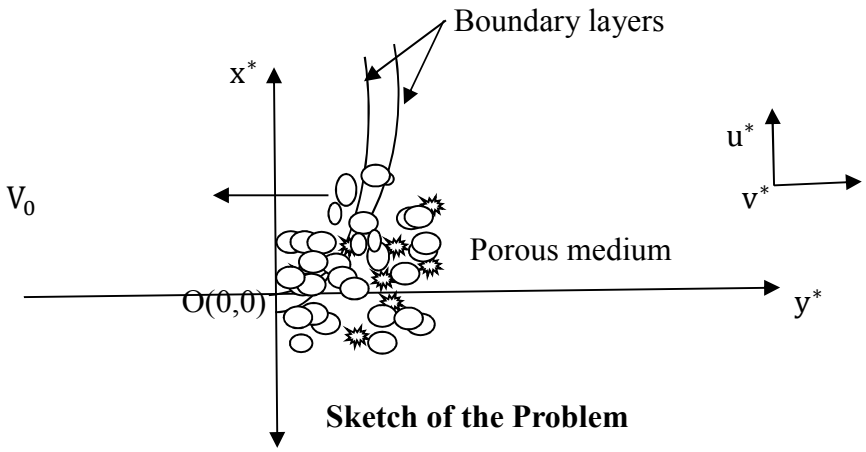

Sketch of the Problem

The governing equations for the problem are (Kim [58], Raptis and Soundalgekar [59], Vyas et al. [60], Raptis [61]):

$$\frac{\partial v^*}{\partial y^*} = 0 \tag{1}$$

The equation of continuity (1) suggests that $v^* = -V_0$

Consequently, the equations of momentum, rotation, and energy respectively become

$$-V_0 \frac{\partial u^*}{\partial y^*} = (\vartheta + \vartheta_r)\frac{\partial^2 u^*}{\partial y^{*2}} + 2\vartheta_r \frac{\partial w^*}{\partial y^*} + g\beta^*(T - T_\infty) - \frac{\vartheta\, u^*}{K^*} \tag{2}$$

$$-\rho J^* V_0 \frac{\partial w^*}{\partial y^*} = \gamma \frac{\partial^2 w^*}{\partial y^{*2}} \tag{3}$$

$$-V_0 \frac{\partial T}{\partial y^*} = \frac{k}{\rho\, c_p}\frac{\partial^2 T}{\partial y^{*2}} + \left(\frac{\vartheta+\vartheta_r}{\rho\, c_p}\right)\left(\frac{\partial u^*}{\partial y^*}\right)^2 + \frac{Q_0}{\rho\, c_p}(T - T_\infty) - \frac{1}{\rho\, c_p}\frac{\partial q_r}{\partial y^*} \tag{4}$$

The boundary conditions are:

$$\left.\begin{array}{c} \text{when } y^* = 0,\ u^* = U_0,\ v^* = -V_0,\ \dfrac{\partial T}{\partial y^*} = -\dfrac{q}{k},\ w^* = -n\dfrac{\partial u^*}{\partial y^*} \\ y^* \to \infty,\ u^* \to 0,\ T \to T_\infty,\ w^* \to 0 \end{array}\right\} \tag{5}$$

where (u^*, v^*) denote velocity components in (x^*, y^*) directions,"ρ; the fluid density", "ϑ; the kinematic viscosity", "ϑ_r; the kinematic rotational viscosity", "β^*; the coefficient of volumetric thermal expansion of the fluid", "K^*; the permeability of the porous medium", "J^*; the microinertia density", "w^*; the component of the angular velocity vector normal to the x^*y^*-plane", "γ; the spin-gradient viscosity", "k; the thermal conductivity", "T; the temperature", "c_p; specific heat at constant pressure", "q; the heat flux", "V_0; the uniform normal velocity".

The boundary condition $w^* = -n\frac{\partial u^*}{\partial y^*}$ describes the relationship between micro rotation variable w^* and the surface stress. The parameter n is micro gyration vector associated with shear stress that

takes values between 0 and 1.

The radiative heat flux q_r in the energy equation is assumed to follow Rosseland approximation (Modest [41]) and is given as

$$q_r = -\frac{4\sigma}{3\delta}\frac{\partial T^4}{\partial y^{*4}} \tag{6}$$

Where σ and δ stand for the Stephan-Boltzman constant and the mean absorption constant respectively. We further assume that the temperature difference in the system is sufficiently small enough so that a Taylor series expansion of T^4 about T_∞ yields

$$T^4 = 4T_\infty^3 T - 3T_\infty^4 \tag{7}$$

We introduce the following non-dimensional quantities:

$$\left.\begin{gathered} u = \frac{u^*}{U_0},\ v = \frac{v^*}{V_0},\ \eta = \frac{V_0 y^*}{\vartheta},\ \theta = \frac{(T-T_\infty)kV_0}{q\,\vartheta},\ w = \frac{\vartheta w^*}{U_0 V_0}, \\ J = \frac{V_0^2 J^*}{\vartheta^2},\ K = \frac{K^* V_0^2}{\vartheta^2},\ q_r = -\frac{4\sigma}{3\delta}\frac{\partial T^4}{\partial y^{*4}}, \end{gathered}\right\} \tag{8}$$

Furthermore, the spin-gradient viscosity γ is given by

$$\gamma = \left(\mu + \frac{\mu_r}{2}\right) = \mu J^*\left(1 + \frac{1}{2}\beta\right), \beta = \frac{\mu_r}{\mu} = \frac{\vartheta_r}{\vartheta} \tag{9}$$

Where β is the non-dimensional viscosity ratio.

In view of the Eq. (9), the governing Eqs. (2)–(4) together with the boundary condition (8) reduce to the following non-dimensional forms

$$(1+\beta)\frac{d^2u}{d\eta^2} + \frac{du}{d\eta} + 2\beta\frac{dw}{d\eta} + Gr\theta - \frac{1}{k}u = 0 \tag{10}$$

$$\frac{d^2w}{d\eta^2} + M\frac{dw}{d\eta} = 0 \tag{11}$$

$$\left(\frac{1+N}{P_r}\right)\frac{d^2\theta}{d\eta^2} + \frac{d\theta}{d\eta} + Q\theta + (1+\beta)Ec\left(\frac{du}{d\eta}\right)^2 = 0 \tag{12}$$

The boundary conditions (5) in the non-dimensional form become

$$\left.\begin{gathered} \eta = 0,\ u = 1, v = -1,\ \frac{d\theta}{d\eta} = -1\,, w = -n\frac{du}{d\eta} \\ \eta \to \infty,\ u \to 0,\ \theta \to 0,\ w \to 0 \end{gathered}\right\} \tag{13}$$

where

$$Gr = \frac{g\beta^* q\vartheta^2}{U_0 V_0^2 k}\ (\text{Grashoff number})$$

$$\beta = \frac{\vartheta_r}{\vartheta}\ (\text{Ratio of viscosity})$$

$$\mathrm{Pr} = \frac{\mu c_p}{k} \text{ (Prandtl number)}$$

$$\mathrm{N} = \frac{16\sigma T_\infty^3}{3\delta k} \text{ (Radiation parameter)}$$

$$\mathrm{Ec} = \frac{U_0^2 V_0}{c_p q \mu} \text{ (Eckert number)}$$

$$\mathrm{Br} = \mathrm{Pr.\ Ec} = \frac{\left(\frac{\vartheta V_0^2}{k}\right)}{\left(\frac{q\vartheta}{U_0 k}\right)} \text{ (Brinkman number)}$$

$$\mathrm{Q} = \frac{Q_0 \mu}{\rho^2 c_p V_0^2} \text{(Suction/injection parameter)}$$

$$\mathrm{M} = \frac{2}{2+\beta}$$

3. Entropy generation

The local volumetric rate of entropy S_G for the configuration under consideration is given as follows (Bejan [36,37], Vyas and Soni [38], Vyas and Shrivastva [39], Shrivastva, Vyas and Soni [40])

$$S_G = \frac{k}{T_\infty^2}\left[\left(\frac{\partial T}{\partial y^*}\right)^2 + \frac{16\sigma T_\infty^3}{3\delta k}\left(\frac{\partial T}{\partial y^*}\right)^2\right] + \frac{\vartheta(1+\beta)}{T_\infty}\left(\frac{\partial u^*}{\partial y^*}\right)^2 + \frac{\vartheta {u^*}^2}{T_\infty K^*} + \frac{\gamma \vartheta^2}{\rho J^* T_\infty V_0^2}\left(\frac{\partial {w^*}^2}{\partial y^*}\right) \tag{14}$$

On prescribing the following characteristic quantities

$$S_{G_0} = \frac{q^2}{T_\infty^2 k} \text{ (the characteristic entropy)}$$

$$\Omega = \frac{T_\infty}{\left(\frac{q\vartheta}{U_0 k}\right)} \text{ (the characteristic temperature ratio)}$$

The entropy generation number Ns is obtained as follows

$$\mathrm{Ns} = \frac{S_G}{S_{G_0}} = [(1+\mathrm{N})\left(\frac{d\theta}{d\eta}\right)^2] + \mathrm{Br}\,\Omega\,[(1+\beta)\left(\frac{du}{d\eta}\right)^2 + \frac{u^2}{K} + \left(1+\frac{\beta}{2}\right)\left(\frac{dw}{d\eta}\right)^2]$$

$$= H_1 + H_2 = \mathrm{HTI} + \mathrm{FFI} \tag{15}$$

Where

$H_1 = (1+\mathrm{N})\left(\frac{d\theta}{d\eta}\right)^2$ stands for the heat transfer irreversibility (HTI),

$H_2 = \mathrm{Br}\,\Omega\left[(1+\beta)\left(\frac{du}{d\eta}\right)^2 + \frac{u^2}{K} + \left(1+\frac{\beta}{2}\right)\left(\frac{dw}{d\eta}\right)^2\right]$ stands for fluid friction irreversibility (FFI),

Further, we define the Bejan Number Be as follows

$$\mathrm{Be} = \frac{\mathrm{HTI}}{\mathrm{HTI+FFI}} \tag{16}$$

4. Solution

In order to solve the governing equations coupled with end conditions, we resorted to the numerical strategy based on finite difference method. Given the coupled nature of the equations concerned, an implicit finite difference method was a suitable choice. The essence of finite difference method is that the solution space $[0,\eta_\infty]$ is discretized into finite number of equispaced mesh points η_j.

$$\eta_j = \eta_0 + jh\,,\ j = 0,1,2,3 \ldots\ldots\ldots N,\ \text{ where the step length } h = \frac{\eta_\infty - \eta_0}{N}.$$

After having the said discretization, the derivatives appearing in the equations and/or in the end conditions are replaced by appropriate finite difference approximations. Similarly, variables are also discretized in the solution space. This discretization reduces the boundary value problem into a system of linear/nonlinear system of algebraic equations that can be handled by suitable numerical method as per the requirement.

In the present case, the employed finite difference scheme yielded a tridiagonal system of linear equations which was solved by Gauss elimination method. The working procedure has been explained as follows.

The boundary value problem [BVP] described by the Eqs. (10) and (12) is coupled and highly nonlinear. For solving the Eqs. (10) and (12), we need solution for w. We resorted to implicit finite difference numerical solution strategy by considering N+1 equispaced grid points.

$$\eta_j = \eta_0 + jh\,,\quad j = 0,1,2,3 \ldots\ldots\ldots N.$$

Further, we denote that $u(\eta_j) = u_j,\ \theta(\eta_j) = \theta_j\ ,\ \ j=0,1,2,3\ldots\ldots N.$ (17)

The equation of angular momentum (11) is an ordinary differential equation and its solution reads

$$w = d + ce^{-M\eta} \tag{18}$$

Where c and d are integration constants and to be determined by the boundary condition (13).
Since, as $\eta \to \infty$, $w = 0$, therefore $d = 0$

Thus, $$w = ce^{-M\eta} \tag{19}$$

Further, when $\eta = 0$, $w = c$. In view of Eq. (13), we get $c = -n\left(\frac{du}{d\eta}\right)_{\eta=0}$. Consequently, Eq. (19) becomes

$$w = -n\left(\frac{du}{d\eta}\right)_{\eta=0} e^{-M\eta}. \tag{20}$$

We discretize $\frac{du}{d\eta}$ as follows

$$\frac{du}{d\eta} = \frac{u_j - u_{j-1}}{h}\ ,\ j= 1,2,3\ldots N - 1.$$

Consequently, $\left(\frac{du}{d\eta}\right)_{\eta=0} = \left(\frac{u_1-u_0}{h}\right)$ leads Eq. (20) to take the following form

$$w = -n\left(\frac{u_1 - u_0}{h}\right)e^{-M\eta}$$

$$w = -n\left(\frac{u_1-1}{h}\right)e^{-M\eta} \qquad (\because\ u_0=1) \tag{21}$$

From the Eq. (21), we note that w would be available if u_1 is known. In order to compute the unknown u_1 a systematic procedure is adopted as described in the ensuing text.

In fact, the Eq. (21) is employed as in (10) and w is nothing but a finite difference approximation involving u_1 with some coefficient.

The essence of the implicit finite difference scheme employed here for u and θ is that both u and θ are refined alternately in a systematic manner by choosing guess values, and the process is initiated first for θ in the solution space. This leads to some approximate solution for u. With this approximated u, the temperature θ is further refined. The process is repeated till the end conditions for both u and θ are satisfied to the prescribed error tolerance of order 10^{-6}.

The BVP has been solved by finite difference method with Gauss elimination iteration scheme for θ. Firstly, the boundary value problem (10) with (13) is solved for u using finite difference scheme for some initial guess value of θ. Then, with this solution for u, the BVP (12) with (13) is solved for further refinement of θ by finite difference method. Here the coefficient matrix is strictly diagonally dominant which is sufficient to ensure that the iterative scheme is convergent for any initial approximation for θ.

In this procedure, the suitable guess values for θ were made by the following reasoning.

Here, we note that the boundary conditions for the temperature θ are

$$\frac{d\theta}{d\eta} = -1 \text{ at } \eta = 0 \text{ and } \theta = 0 \text{ at } \eta \to \infty \tag{22}$$

Hence we can go for approximating θ by taking

$$\theta_j = e^{-\eta_j}\ , j = 0,1,2,3, \dots \dots \dots N-1 \qquad \text{and } \theta_N = e^{-\eta_N} = 0 \tag{23}$$

keeping the above end conditions for θ into account.

For solving the Eq. (10) under the associated boundary conditions, an implicit finite difference scheme has been developed. Assuming the following finite difference approximations

$$\frac{d^2u}{d\eta^2} = \frac{u_{j+1}-2u_j+u_{j-1}}{h^2}, \qquad \frac{d^2\theta}{d\eta^2} = \frac{\theta_{j+1}-2\theta_j+\theta_{j-1}}{h^2} \tag{24}$$

$$\frac{du}{d\eta} = \frac{u_j-u_{j-1}}{h}, \qquad \frac{d\theta}{d\eta} = \frac{\theta_j-\theta_{j-1}}{h} \tag{25}$$

$$u = \frac{u_j+u_{j-1}}{2}, \qquad \theta = \frac{\theta_j+\theta_{j-1}}{2} \tag{26}$$

Then the differential Eq. (10) is discretized with the Eq. (21) as follows:

$$(1+\beta)\left(\frac{u_{j+1}-2u_j+u_{j-1}}{h^2}\right) + \left(\frac{u_j-u_{j-1}}{h}\right) + 2\beta\frac{nM}{h}(u_1-1)e^{M\eta_j} - \frac{1}{k}\left(\frac{u_j+u_{j-1}}{2}\right) + Gr\left(\frac{\theta_j+\theta_{j-1}}{2}\right) = 0$$

Which on rearranging terms takes the form

$$\left.\begin{aligned}\left(\frac{1+\beta}{h^2}\right)u_{j+1}+\left(\frac{1}{h}-\frac{1}{2k}-\frac{2(1+\beta)}{h^2}\right)u_j+\left(\frac{1+\beta}{h^2}-\frac{1}{h}-\frac{1}{2k}\right)u_{j-1}+2\frac{\beta nM}{h}e^{-M\eta_j}u_1\\ =2\frac{\beta nM}{h}e^{-M\eta_j}-Gr\left(\frac{\theta_j+\theta_{j-1}}{2}\right),\ j=1,2,3,\dots\dots\dots\dots N-1.\end{aligned}\right\} \quad (27)$$

The end condition $\eta\to\infty,\ u\to 0$ is discretized as
$u=[u_1\quad u_2\ u_3\quad u_4\cdots\cdots u_{N-1}\quad u_N]$. Consequently, $u_N=0$ can be written as

$$0.u_1+0.u_2+0.u_3+\cdots\dots\dots\dots\dots\dots 1.u_N=0 \quad (28)$$

The Eqs. (27) and (28) lead to the system of linear equations which, in matrix form reads

$$\begin{bmatrix}C_2+C_4(1) & C_3 & 0 & 0 & \cdots & 0 & 0 & 0 & 0\\ C_1+C_4(2) & C_2 & C_3 & 0 & \cdots & 0 & 0 & 0 & 0\\ C_4(3) & C_1 & C_2 & C_3 & \cdots & 0 & 0 & 0 & 0\\ \vdots & \vdots & \vdots & \vdots & \ddots & \vdots & \vdots & \vdots & \vdots\\ C_4(N-2) & 0 & 0 & 0 & \cdots & C_1 & C_2 & C_3 & 0\\ C_4(N-1) & 0 & 0 & 0 & \cdots & 0 & C_1 & C_2 & C_3\\ 0 & 0 & 0 & 0 & \cdots & 0 & 0 & 0 & 1\end{bmatrix}_{N\times N}\begin{bmatrix}u_1\\ u_2\\ u_3\\ \vdots\\ u_{N-2}\\ u_{N-1}\\ u_N\end{bmatrix}_{N\times 1}=\begin{bmatrix}B_1\\ B_2\\ B_3\\ \vdots\\ B_{N-2}\\ B_{N-1}\\ 0\end{bmatrix}_{N\times 1} \quad (29)$$

where

$$\left.\begin{aligned}C_1=\left(\frac{1+\beta}{h^2}-\frac{1}{h}-\frac{1}{2k}\right),\ C_2=\left(\frac{1}{h}-\frac{1}{2k}-\frac{2(1+\beta)}{h^2}\right),\ C_3=\left(\frac{1+\beta}{h^2}\right),\\ C_4(j)=2\frac{\beta nM}{h}e^{-M\eta_j},\quad B_1=C_4(1)-Gr\left(\frac{\theta_1+\theta_0}{2}\right)-C_1,\\ B_j=C_4(j)-Gr\left(\frac{\theta_j+\theta_{j-1}}{2}\right),\ j=2,3,4,\dots N-1,\end{aligned}\right\} \quad (30)$$

Now on employing Gauss elimination method in the matrix given by Eq. (29), we get the solution $[u_1\quad u_2\ u_3\quad u_4\cdots\cdots\cdots u_{N-1}\quad u_N]^T$.

Hence, by including the given initial boundary condition for u, we obtain the complete solution for the velocity u corresponding to chosen guess value of θ as follows

$$u=[u_0\quad u_1\quad u_2\quad u_3\quad\cdots\quad\cdots\quad\cdots\quad u_{N-2}\quad u_{N-1}\quad u_N]^T.$$

This solution is then employed into the Eq. (12) to seek further refined value of θ that was guessed earlier.

Now we discretize the Eq. (12) by employing the finite difference approximations as follows:

$$\left(\frac{1+N}{Pr}\right)\left(\frac{\theta_{j+1}-2\theta_j+\theta_{j-1}}{h^2}\right)+\left(\frac{\theta_j-\theta_{j-1}}{h}\right)+Q\left(\frac{\theta_j+\theta_{j-1}}{2}\right)\theta_j=-(1+\beta)Ec\left(\frac{u_j-u_{j-1}}{h}\right)^2$$

Which on rearranging terms takes the form

$$\left.\begin{aligned}\left(\frac{1+N}{Pr}\right)\theta_{j+1}+\left(h-\frac{2(1+N)}{Pr}+Qh^2\right)\theta_j+\left(\frac{1+N}{Pr}-h+Qh^2\right)\theta_{j-1}=-(1+\beta)Ec\left(u_j-u_{j-1}\right)^2\\ j=1,2,3,\dots.N-1,\end{aligned}\right\} \quad (31)$$

Now from Eq. (22) we have

$$\theta'(0)=-1\implies\quad\frac{\theta_1-\theta_0}{h}=-1 \quad (32)$$

Then, the system of linear equations for $\theta_j's$ is

$$\left.\begin{gathered}\theta_0 - \theta_1 = h \\ \left(\frac{1+N}{Pr}\right)\theta_{j+1} + \left(h - \frac{2(1+N)}{Pr} + Qh^2\right)\theta_j + \left(\frac{1+N}{Pr} - h + Qh^2\right)\theta_{j-1} = -(1+\beta)Ec\left(u_j - u_{j-1}\right)^2 \\ j = 1,2,3,\ldots\ldots N-1\end{gathered}\right\} \quad (33)$$

Which, in matrix form, is written as

$$\begin{bmatrix} 1 & -1 & 0 & 0 & \cdots & 0 & 0 & 0 & 0 \\ C_5 & C_6 & C_7 & 0 & \cdots & 0 & 0 & 0 & 0 \\ 0 & C_5 & C_6 & C_7 & \cdots & 0 & 0 & 0 & 0 \\ 0 & 0 & C_5 & C_6 & \cdots & 0 & 0 & 0 & 0 \\ \cdots & \cdots & \cdots & \vdots & \ddots & \vdots & \cdots & \cdots & \cdots \\ 0 & 0 & 0 & 0 & \cdots & C_5 & C_6 & C_7 & 0 \\ 0 & 0 & 0 & 0 & \cdots & 0 & C_5 & C_6 & C_7 \\ 0 & 0 & 0 & 0 & \cdots & 0 & 0 & C_5 & C_6 \end{bmatrix}_{N\times N} \begin{bmatrix} \theta_0 \\ \theta_1 \\ \theta_2 \\ \vdots \\ \theta_{N-3} \\ \theta_{N-2} \\ \theta_{N-1} \end{bmatrix}_{N\times 1} = \begin{bmatrix} T_0 \\ T_1 \\ T_2 \\ \vdots \\ T_{N-3} \\ T_{N-2} \\ T_{N-1} \end{bmatrix}_{N\times 1} \quad (34)$$

where

$$\left.\begin{gathered} C_5 = \frac{(1+N)}{Pr} - h + Qh^2, \quad C_6 = h - \frac{2(1+N)}{Pr} + Qh^2, \quad C_7 = \frac{1+N}{Pr}, \\ T_0 = h, \quad T_j = -(1+\beta)Ec\left(u_j - u_{j-1}\right)^2, \quad j = 1,2,3\ldots\ldots\ldots\ldots N-1 \end{gathered}\right\} \quad (35)$$

Equation (34) is then solved by Gauss elimination method to yield $\theta_j's$. With these currently approximated $\theta_j's$,we now again solve Eq. (10) in the quest for better u. The process is continued until $\left|u^{k+1} - u^k\right| < 10^{-6}$ and $\left|\theta^{k+1} - \theta^k\right| < 10^{-6}$ criterion is achieved.

Here we would like to make a remark that the computational procedure was very rigorous in the sense that estimation of unknown quantities and their refinement to desired accuracy proved to be really painstaking owing to immense non-linear nature of the problem. In order to terminate the refinement process, the error tolerance was taken as $\in = 10^{-6}$. These computations provided numerical solution to momentum and thermal regime which were readily used to compute entropy.

Interested readers may also refer to Altan and El-Mikkawy [62], Jiteng and Li [63] for a good insight on a new algorithm for general opposite-bordered tridiagonal (OBT) linear systems.

5. Results and discussion

The computed quantities w, u and θ and their gradients are employed to evaluate entropy generation number to provide plots for entropy generation number and Bejan number.

The Figure 1 depicts that N_S decreases with increasing values of heat sink parameter Q. The rising values of Q indicate heat being poured out of the system. The information is of paramount application in thermal optimization in electronic devices which use heat sinks. The Figure 2 displays that the Bejan Number Be has peaks in the vicinity of the moving plate, and as we move farther away from the plate then the Bejan number tends to vanish. We also see that the Bejan number has higher peaks for larger values of heat sink parameter Q. Furthermore, the trend of Bejan number variations for varying values of Q is not uniform across the boundary layer. The Bejan number Be increases in the vicinity of the plate with increasing values of Q, however the trend is reversed at some spatial distance in the

boundary layer. It may be attributed to the fact the larger values of Q amount to pronounced transfer of heat thereby causing rise in the heat transfer irreversibility. The Figure 3 shows entropy N_S decreases for increasing values of radiation parameter N. The Figure 4 reveals that The Bejan number Be increases in the vicinity of the plate with increasing values of radiation parameter N, however the trend is reversed at some spatial distance in the boundary layer. The Figure 5 demonstrates that entropy number N_S increases with the increasing values of Grashoff number Gr that accounts for the buoyancy. The Figure 6 depicting variations in Be shows that the Bejan number Be increases across the boundary layer for increasing values of Grashoff number Gr, and it attains peaks in the vicinity of the plate. The Figure 7 demonstrates the rise in N_S for increasing values of Brinkman number. The higher values of Br stand for more pronounced frictional heat in the system there by causing a rise in entropy generation. However, the Bejan number decays for increasing Br values as is evident from the Figure 8.

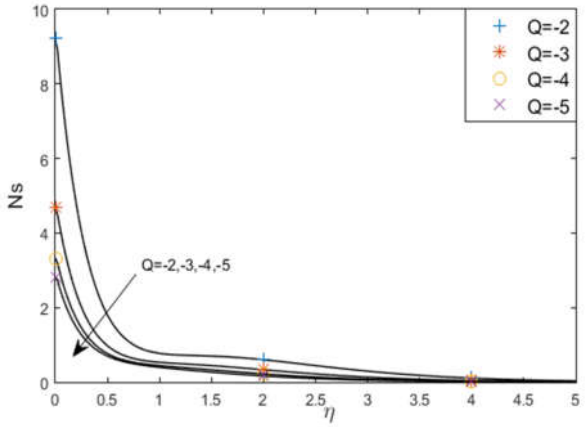

Figure 1. Plots for N_S versus **η** as varying Suction parameter Q for β = 0.5, n = 0.5, K=10, Pr =1, N=1.5, Gr = 4, Ec = 0.05, Ω= 0.5, Br = 1.

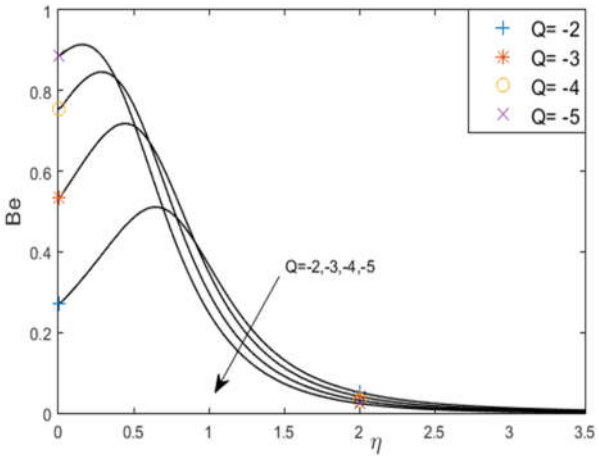

Figure 2. Plots for Be versus **η** as varying Suction parameter Q for β = 0.5, n = 0.5, K=10, Pr = 1, N=1.5, Gr=4, Ec = 0.05, Ω= 0.5, Br = 1.

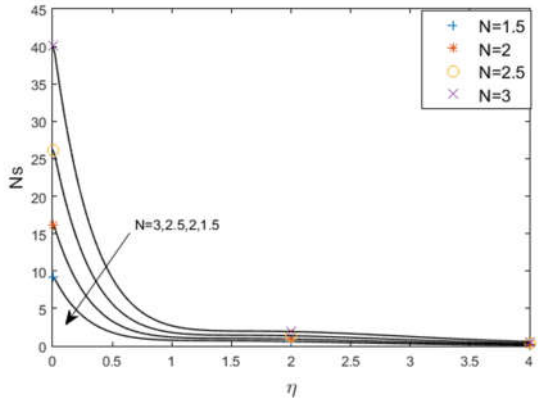

Figure 3. Plots for Be versus **η** as varying Radiation parameter N for β =0.5, n=0.5, K=10, Pr=1, Q = −2, Gr=4, Ec = 0.05, Ω=0.5, Br =1.

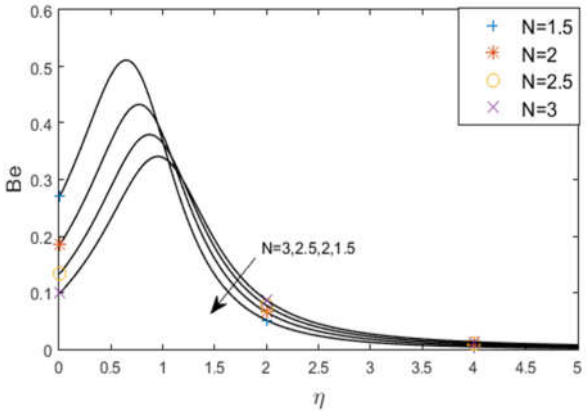

Figure 4. Plots for Be versus **η** as varying Radiation parameter N for β = 0.5, n=0.5, K=10, Pr = 1, Q = −2, Gr = 4, Ec = 0.05, Ω = 0.5, Br = 1.

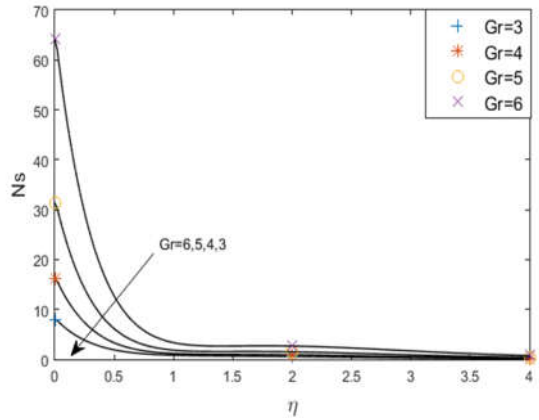

Figure 5. Plots for N_S versus **η** as varying Groshoff Number Gr for β = 0.5, n = 0.5, K=10, Pr =1, Q = −2, N = 2, Ec = 0.05, Ω= 0.5, Br=1.

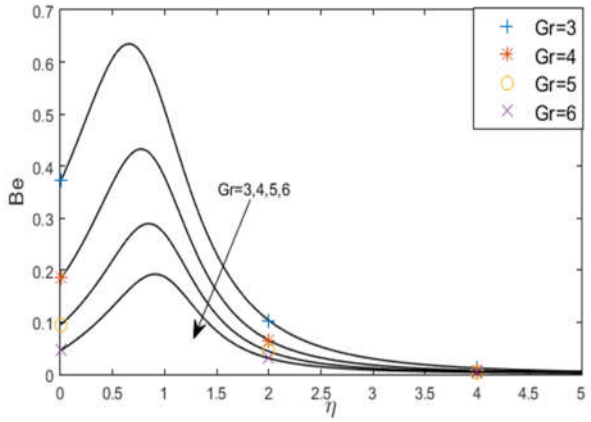

Figure 6. Plots for Be versus **η** as varying Groshoff Number Gr for β = 0.5, n = 0.5, K = 10,Pr = 1,Q = −2, N = 2, Ec = 0.05, Ω= 0.5, Br=1.

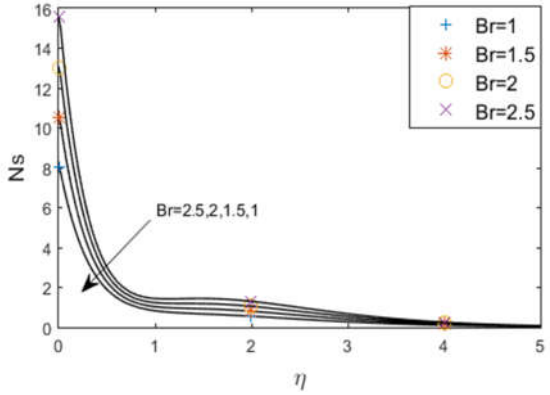

Figure 7. Plots for N_S versus **η** as varying Brinkmann number Br for β = 0.5, n = 0.5, K=10, Q = −2, Gr = 3, N = 2, Ω = 0.5.

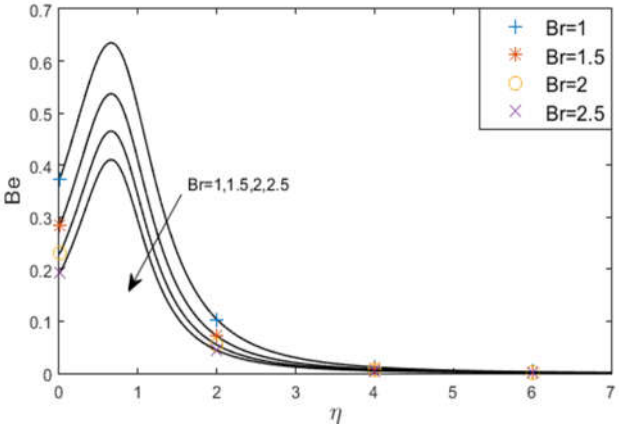

Figure 8. Plots for Be versus **η** as varying Brinkmann number Br for β = 0.5, n = 0.5, K=10, Q = −2, Gr=3, N=2, Ω= 0.5.

6. Conclusion

Entropy generation analysis for boundary layer flow in a porous medium saturated with micropolar fluid, was considered. The flow was assumed to be caused due to a vertically moving plate perfectly attached with porous medium and buoyancy. The mathematical model solved numerically led to a convergent system of linear equations. First the velocity, temperature and microrotation were computed, secondly these quantities and their gradients, were employed to compute entropy. The plots for entropy Ns and the Bejan number Be were drawn to give insight about the effect of the parameters entering in to the problem. it was found that the parameters have qualitative and quantitative effects on the quantities of interest. In fact, the entropy generation analysis (EGA) is an instrumental exercise for entropy generation minimization (EGM). The novelty of the problem is that it involves an efficient numerical method with a reasonably good error tolerance for wide range of parameters values. Besides the numerical procedure, the thermofluidics considered here has ample applications where in the configurations may exist as a single independent unit or may be a part of some larger setup. The study may find applications in chemical, automobile and other industries where varied polymeric suspensions, lubricants, paints, colloids, body fluids, poly-liquids, liquid foams, polymeric additives, liquid crystals, sediments etc. can be viewed as micropolar fluid. The main findings of the problem are:

1) N_S decreases with increasing values of heat sink parameter Q, radiation parameter N.
2) N_S increases with increasing values of Grashoff number Gr, brinkman number Br.
3) The Bejan number shows pronounced variations for the parameters entering into the problem.
4) The presented entropy generation analysis (EGA) may be instrumental for future endeavor of entropy generation minimization(EGM).

Acknowledgments

The authors are indebted to the learned reviewers for their valuable comments, which led to considerable improvement of the paper.

Conflict of interest

All authors declare no conflicts of interest in this paper.

References

1. A. C. Eringen, *Theory of micropolar fluids*, J. Math. Mech., **16** (1966), 1–18.
2. A. C. Eringen, *Theory of thermomicrofluids*, J. Math. Anal. Appl., **38** (1966), 480–496.
3. M. M. Khonsari, *On the self-excited whirl orbits of a journal in a sleeve, bearing lubricated with micropolar fluids*, Acta Mech., **81** (1990), 235–244.
4. M. M. Khonsari, D. Brewe, *On the performance of finite journal bearing lubricated with micropolar fluids*, STLE Tribol. Transm., **32** (1989), 155–160.
5. B. Hadimoto, T. Tokioka, *Two-dimensional shear flows of linear micropolar fluids*, Int. J. Eng. Sci., 7 (1969), 515–522.
6. F. Lockwood, M. Benchaita, S. Friberg, *Study of polyotropic liquid crystals in viscometric flow and elasto hydrodynamic contact*, ASLE Tribol. Transm., **30** (1987), 539–548.

7. J. D. Lee, A. C. Eringen, *Boundary effects of orientation of nematic liquid crystals*, J. Chem. Phys., **55** (1971), 509–512.
8. V. Kolpashchikov, N. P. Migun, P. P. Prokhorenko, *Experimental determinations of material micropolar coefficients*, Int. J. Eng. Sci., **21** (1983), 405–411.
9. T. Ariman, M. A. Turk, N. D. Sylvester, *Micro continuum fluid mechanics: A review*, Int. J. Eng. Sci., 11 (1973), 905–930.
10. T. Ariman, M. A. Turk, N. D. Sylvester, *Application of micro continuum fluid mechanics*, Int. J. Eng. Sci., **12** (1974), 273–293.
11. G. Ahmedi, *Self-similar solution of incompressible micropolar boundary layer flow over a semi-infinite plate*, Int. J. Eng. Sci., **14** (1976), 639–646.
12. S. K. Jena, M. N. Mathur, *Free convection in the laminar boundary layer flow of thermomicropolar fluid past a non-isothermal vertical flat plate with suction/injection*, Acta Mech., **42** (1982), 227–238.
13. E. M. Abo-Eldahab, M. A. El-Aziz, *Flow and heat transfer in a micropolar fluid past a stretching surface embedded in a non-Darcian porous medium with uniform free stream*, Appl. Math. Comput., **162** (2005), 881–899.
14. M. M. Rashidi, N. Kavyani, S. Abelman, *Investigation of entropy generation in MHD and slip flowover a rotating porous disk with variable properties*, Int. J. Heat Mass Tran., **70** (2014), 892–917.
15. D. Gupta, L. Kumar, O. A. Bég, et al. *Finite element simulation of mixed convection flow of micropolar fluid over a shrinking sheet with thermal radiation*, P. I. Mech. Eng. E, **228** (2014), 61–72.
16. N. Ali, A. Zaman, O. A. Bég, *Numerical simulation of unsteady micropolar hemodynamics in a tapered catheterized artery with a combination of stenosis and aneurysm*, Med. Biol. Eng. Comput., **54** (2015), 1423–1436.
17. M. J. Uddin, M. N. Kabir, Y. M. Alginahi, *Lie group analysis and numerical solution of magnetohydrodynamic free convective slip flow of micropolar fluid over a moving plate with heat transfer*, Comput. Math. Appl., **70** (2015), 846–856.
18. I. Dražić, N. Črnjarić-Žic, L. Simčić, *A shear flow problem for compressible viscous micropolar fluid: Derivation of the model and numerical solution*, Math. Comput. Simulat., **162** (2019), 249–267.
19. A. A. Farooq, D. Tripathib, T. Elnaqeeb, *On the propulsion of micropolar fluid inside a channel due to ciliary induced metachronal wave*, Appl. Math. Comput., **347** (2019), 225–235.
20. H. H. Sherief, M. S. Faltas, S. El-Sapa, *Interaction between two rigid spheres moving in a micropolar fluid with slip surfaces*, J. Mol. Liq., **290** (2019), 111165.
21. M. S. Uddin, K. Bhattacharyya, S. Shafie, *Micropolar fluid flow and heat transfer over an exponentially permeable shrinking sheet*, Popul. Power Res., **5** (2016), 310–317.
22. R. D. Cess, *The Interaction of thermal radiation with free convection heat transfer*, Int. J. Heat Mass Tran., **9** (1966), 1269–1277.
23. A. A. Hayday, D. A. Bowlus, R. A. McGraw, *Free convection from a vertical flat plate with step discontinuities in surface temperature*, ASME J. Heat Tran., **89** (1967), 244–250.
24. T. T. Kao, *Laminar free convective heat transfer response along a vertical plat plate with step jump in surface temperature*, Heat Mass Transfer, **2** (1975), 419–428.

25. P. Cheng, W. J. Minkowycz, *Flow about a vertical flat plate embedded in a porous medium with application to heat transfer from a dike*, J. Geophys. Res., **82** (1977), 2040–2044.
26. A. Raptis, N. Kafousias, *Heat transfer in flow through a porous medium bounded by an infinite vertical plate under the action of a magnetic field*, Energy Res., **6** (1982), 241–245.
27. M. V. A. Bianchi, R. Viskanta, *Momentum and heat transfer on a continuous flat surface moving in a parallel counterflow free stream*, Warme-und Stoffubertrangung, **29** (1993), 89–94.
28. H. S. Thakhar, R. S. R. Gorla, V. M. Soundalgekar, *Radiation effect on MHD free convection flow of a radiating gas past a semi-infinite vertical plate*, Int. J. Numer. Method Heat, **6** (1996), 77–83.
29. A. J. Chamkha, *Unsteady MHD convective heat and mass transfer past a semi-infinite vertical permeable moving plate with heat absorption*, Int. J. Eng. Sci., **24** (2004), 217–230.
30. M. M. Abdelkhalek, *Heat and Mass transfer in MHD free convection from a moving permeable vertical surface by a perturbation technique*, Commun. Nonlinear Sci., **14** (2009), 2091–2102.
31. O. D. Makinde, *Similarity solution for natural convection from a moving vertical plate with internal heat generation and a convective boundary condition*, Therm. Sci., **15** (2011), 5137–5143.
32. D. Srinivasacharya, O. Surender, *Non-similar solution for natural convective boundary layer flow of ananofluid past a vertical plate embedded in a doubly stratified porous medium*, Int. J. Heat Mass Tran., **71** (2014), 431–438.
33. A. Khalid, I. Khan, S. Shafie, *Heat transfer in ferrofluid with cylindrical shape nanoparticles past a vertical plate with ramped wall temperature embedded in a porous medium*, J. Mol. Liq., **221** (2016), 1175–1183.
34. S. R. Mishra, I. Khanb, Q. M. Al-mdallalc, et al. *Free convective micropolar fluid flow and heat transfer over a shrinking sheet with heat source*, Case Stud. Therm. Eng., **11** (2018), 113–119.
35. H. Chen, J. Ma, H. Liu, *Least square spectral collocation method for nonlinear heat transfer in moving porous plate with convective and radiative boundary conditions*, Int. J. Therm. Sci., **132** (2018), 335–343.
36. A. Bejan, *A study of entropy generation in fundamental convective heat transfer*, J. Heat Trans., **101** (1979), 718–725.
37. A. Bejan, *Second law analysis in heat transfer*, Energy, **5** (1980), 721–732.
38. P. Vyas, S. Soni, *Entropy analysis for MHD casson fluid flow in a channel subjected to weakly temperature dependent convection coefficient and hyderodynamic slip*, J. Rajasthan Acad. Phys. Sci., **15** (2016), 1–18.
39. P. Vyas, N. Srivastava, *Entropy analysis of generalized MHD Couette flow inside a composite duct with asymmetric convective cooling*, Arab. J. Sci. Eng., **40** (2015), 603–614.
40. N. Srivastava, P. Vyas, S. Soni, *Entropy generation analysis for oscillatory flow in a vertical channel filled with Porous Medium*, IEEE International Conference on Recent Advances and Innovations in Engineering (ICRAIE-2016), December 23-25, Jaipur, India.
41. M. F. Modest, *Heat Transfer,* 2 Eds., Academic press, 2003.
42. D. Srinivasacharya, K. H. Bindu, *Entropy generation due to micropolar fluid flow between concentric cylinders with slip and convective boundary conditions*, Ain Shams Eng. J., **9** (2018), 245–255.
43. D. Srinivasacharya, K. H. Bindu, *Entropy generation of micropolar fluid flow in an inclined porous pipe with convective boundary conditions*, Sadhna, **42** (2017), 729–740.

44. S. K. Asha, C. K. Deepa, *Entropy generation for peristaltic blood flow of a magneto-micropolar fluid with thermal radiation in a tapered asymmetric channel*, Results Eng., **3** (2019), 100024.
45. A. Z. Sahin, *Second law analysis of laminar viscous flow through a duct subjected to constant wall temperature*, J. Heat Trans., **120** (1998), 76–83.
46. J. V. R. Murthy, J. Srinivas, *Second law analysis for Poiseuille flow of immiscible micropolar fluids in a channel*, Int. J. Heat Mass Tran., **65** (2013), 254–264.
47. C. K. Chen, Y. T. Yang, K. H. Chang, *The effect of thermal radiation on entropy generation due to micro-polar fluid flow along a wavy surface*, Entropy, **13** (2011),1595–1610.
48. A. Shahsavar, P. T. Sardari, D. Toghraie, *Free convection heat transfer and entropy generation analysis of water-Fe3O4/CNT hybridnanofluid in a concentric annulus*, Int. J. Numer. Meth. Heat Fluid Flow, **424** (2018), 0961–5539.
49. E. Manay, E. F. Akyürek, B. Sahin, *Entropy generation of nanofluid flow in a microchannel heat sink*, Results Phys., **9** (2018), 615–624.
50. P. Barnoon, D. Toghrai, R. B. Dehkordi, et al. *MHD mixed convection and entropy generation in a lid-driven cavity with rotating cylinders filled by a nanofluid using two phase mixture model*, J. Magn. Magn. Mater., **483** (2019), 224–248.
51. P. Barnoon, D. Toghraie, F. Eslami, et al. *Entropy generation analysis of different nanofluid flows in the space between two concentric horizontal pipes in the presence of magnetic field: Single-phase and two-phase approaches*, Comput. Math. Appl., **73** (2019), 662–692.
52. A. A. A. A. Abdullah, O. A. Akbari, A. Heydari, et al. *The numerical modeling of water/FMWCNT nanofluid flow and heat transfer in a backward-facing contracting channel*, Physica B, **537** (2018), 176–183.
53. S. M. Seyyedi, A. S. Hashemi-Tilehnoee, M. Waqas, et al. *Entropy generation and economic analyses in a nanofluid filled L-shaped enclosure subjected to an oriented magnetic field*, Appl. Therm. Eng., **168** (2019), 114789.
54. M. Maskaniyan, M. Nazari, S. Rashidi, et al. *Natural convection and entropy generation analysis inside a channel with a porous plate mounted as a cooling system*, Therm. Sci. Eng. Prog., **6** (2018),186–193.
55. P. Gholamalipour, M. Siavashi, M. H. Doranehgard, *Eccentricity effects of heat source inside a porous annulus on the natural convection heat transfer and entropy generation of Cu-water nanofluid*, Int. Commun. Heat Mass Tran., **109** (2019), 104367.
56. P. Vyas, S. Khan, *Entropy analysis for MHD dissipative Casson fluid flow in porous medium due to stretching cylinder*, Acta Tech., **61** (2016), 299–315.
57. P. Vyas, N. Srivastava, *Entropy analysis for magnetohyrodynamic fluid flow in porous medium due to a non-isothermal stretching sheet*, J. Rajasthan Acad. Phys. Sci.,**14** (2015), 323–336.
58. Y. J. Kim, *Heat and mass transfer in MHD micropolar flow over a vertical moving porous plate in a porous medium*, Transport in Porous Med., **56** (2004), 17–37.
59. A. A. Raptis, V. M. Soundalgekar, *MHD flow past a steadily moving infinite vertical porous plate with constant heat flux*, Nucl. Eng. Des., **72** (1982), 373–379.
60. P. Vyas, A. Rai, K. S. Shekhawat, *Dissipative heat and mass transfer in porous medium due to continuously moving plate*, Appl. Math. Sci., **6** (2012), 4319–4330.
61. A. A. Raptis, *Flow of a micropolar fluid past a continuously moving plate by the presence of rotation*, Int. J. Heat Mass Tran., **41** (1998), 2865–2866.

62. F. Atlan, M. E. A. El-Mikkawy, *A new symbolic algorithm for solving general opposite-bordered tridiagonal linear systems*, Am. J. Comput. Math., **5** (2015), 258–266.
63. J. Jia, S. Li, *New algorithms for numerically solving a class of bordered tridiagonal systems of linear equations*, Comput. Math. Appl., **78** (2019), 144–151.

AIMS Press